PROCEEDINGS B

royalsocietypublishing.org/journal/rspb

Research

Cite this article: Eliason CM, Clarke JA. 2018 Metabolic physiology explains macroevolutionary trends in the melanic colour system across amniotes. *Proc. R. Soc. B* **285**: 20182014.
http://dx.doi.org/10.1098/rspb.2018.2014

Received: 6 September 2018
Accepted: 21 November 2018

Subject Category:
Evolution

Subject Areas:
evolution

Keywords:
melanosome, phenotypic evolution, Brownian motion

Author for correspondence:
Chad M. Eliason
e-mail: cme16@zips.uakron.edu

Electronic supplementary material is available online at https://dx.doi.org/10.6084/m9.figshare.c.4320842.

THE ROYAL SOCIETY PUBLISHING

Metabolic physiology explains macroevolutionary trends in the melanic colour system across amniotes

Chad M. Eliason[1,2] and Julia A. Clarke[2]

[1]Integrative Research Center, Field Museum of Natural History, Chicago, IL, USA
[2]Jackson School of Geosciences, University of Texas at Austin, Austin, TX, USA

CME, 0000-0002-8426-0373

Metabolism links organisms to their environment through its effects on thermoregulation, feeding behaviour and energetics. Genes involved in metabolic processes have known pleiotropic effects on some melanic colour traits. Understanding links between physiology and melanic colour is critical for understanding the role of, and potential constraints on, colour production. Despite considerable variation in metabolic rates and presumed ancestral melanic coloration in vertebrates, few studies have looked at a potential relationship between these two systems in a comparative framework. Here, we test the hypothesis that changes in melanosome shape in integumentary structures track metabolic rate variation across amniotes. Using multivariate comparative analyses and incorporating both extant and fossil taxa, we find significantly faster rates of melanosome shape evolution in taxa with high metabolic rates, as well as both colour- and clade-specific differences in the relationship between metabolic rate and melanosome shape. Phylogenetic tests recover an expansion in melanosome morphospace in maniraptoran dinosaurs, as well as rate shifts within birds (in songbirds) and mammals. These findings indicate another core phenotype influenced by metabolic changes in vertebrates. They also provide a framework for testing clade-specific gene expression patterns in the melanocortin system and may improve colour reconstructions in extinct taxa.

1. Background

Organisms are integrated across genetic, developmental, functional and phenotypic levels [1]. Understanding how traits may be correlated or linked is critical for understanding evolutionary trends and selective regimes affecting one or more of these traits [2]. Colour provides an integrative framework [3] for testing how trait correlations might drive macroevolutionary trends. Melanic colour, the most ubiquitous form of coloration in animals [4], is regulated primarily by the melanocortin system—a suite of melanocortin hormones, melanocortin receptors and antagonists that together affect colour as well as organismal behaviour and physiology [5]. Pleiotropy within the melanocortin system has been well studied at the population level (reviewed in [5,6]) and is proposed to explain links between melanic colour and other organismal traits, including body mass [7], social behaviour [8], diet and energetics [9] and metabolic rate [10]. However, few studies have investigated links between melanic colour and metabolism in a comparative framework or asked how aspects of the melanic colour system itself may evolve with major shifts in energetics [11]. Studying macroevolutionary trends within the melanocortin system is critical for understanding potential constraints on colour evolution and identifying mechanisms underlying the repeated evolution of links between colour and other phenotypic traits in vertebrates [6].

Melanin pigments, including yellow to reddish-brown phaeomelanin and dark brown to black eumelanin [4], are contained in organelles known as melanosomes. Different forms of melanin have distinct metabolic pathways [12] and may be differentially associated with some physiological traits (e.g. oxidative stress) [13].

Observed relationships between colour and melanosome shape (e.g. round phaeomelanosomes and cylindrical eumelanosomes) [14] probably stem from changes in genes influencing both melanin chemistry and melanosome shape [15–17]. Melanin pigment genes (e.g. *POMC*) evolve faster in species with higher metabolic rates [18]. Qualitative studies at broader taxonomic scales have also recovered evidence for decreased melanosome shape disparity in heterotherms compared to homeotherms [19] and in extant large-bodied, flightless birds relative to volant taxa with higher metabolic rates [20]. These results have been used to propose a role for the pleiotropic effects of the melanocortin system to explain these patterns at a macroevolutionary scale [19,20]. However, this hypothesis has not been tested in a quantitative and comparative framework.

Here, we ask whether metabolic physiology explains shifts in the melanic colour system across amniotes. Specifically, we hypothesize that pleiotropic interactions within the melanocortin system [5] may cause covariation between metabolic physiology and one melanin trait, melanosome shape. We tested the following three predictions: (i) metabolic rates will be associated with increased rates of melanosome shape evolution; (ii) melanosome shape will relate to metabolic rate differently for eumelanin-consistent (black or grey) and phaeomelanin-consistent (yellow or reddish-brown) integumentary colours; and (iii) the relationship between metabolism and melanosome shape will vary among subclades. We test these predictions derived from prior qualitative studies [19,20] using a large synthetic dataset in a multivariate comparative framework. Our results have implications for estimating colour in extinct species and set the stage for further work on the genetic underpinnings of clade-specific trends in the melanic colour system across vertebrates.

2. Material and methods

(a) Melanosome morphology

We used published data for melanosome length and diameter measured from scanning electron microscope images [19,21]. These measurements were taken from integument cross-sections for various integumentary structures (feathers, hairs, scales) of known colour (e.g. grey, brown, black). Briefly, cross-sections were prepared in previous work by embedding samples in resin, slicing blocks into 5 µm-thick cross-sections with a microtome and imaging the cross-sections on a scanning electron microscope. Images were analysed and measured in ImageJ to obtain the lengths along the short axis (diameter) and long axis (length) for several melanosomes per sample. We also took length and width measurements for melanosomes ($n = 10$) in a fossil frog from the Miocene based on published images [22].

(b) Metabolic rates and body size

We used available vetted data on metabolic rates in amniotes [23,24]. Hereafter, we use 'metabolic rate' to refer to both basal (BMR, for homeotherms) and standard metabolic rates (SMR, for heterotherms) for non-avian reptiles (lizards, snakes) [23]. Since metabolic rate varies during feeding or movement, standard metabolic rate (SMR, measured in resting, non-growing animals) is typically used in the literature [25]. For homeothermic animals that further regulate their body temperatures (e.g. mammals and birds), basal metabolic rate defines the 'lower limit of metabolic heat production' [23]. Since body size increases strongly with metabolic rate [25], we computed mass-specific metabolic rates by dividing metabolic rates (measured in watts) by body mass (measured in grams) and then log-transforming these values. For 170 (66%) species without metabolic rate data, we obtained body masses from published sources for birds [26], mammals [27], and non-avian reptiles [28], normalized SMR for heterothermic taxa [25], and calculated mass-derived metabolic rates using published taxon-specific regression values derived from a much larger dataset across domains of life [25]. All variables were ln-transformed before analysis.

(c) Phylogeny

We combined recent supertrees for non-avian reptiles [29], mammals [11] and birds [30] (with branch lengths from [31]) into a synthetic amniote supertree. We stitched time-calibrated supertrees together using the bind.tip function in phytools [32] based on published divergence times [33] among the three major clades. We then added 20 species with trait data but not represented in the final tree using the add species to genus function in phytools [32]. This conservative approach adds species as a polytomy to the most recent common ancestor of all congeneric species. The final extant supertree contained 15 423 extant species, to which we added 19 additional fossil taxa (see electronic supplementary material, methods and table S1 for details).

(d) Comparative analyses

(i) Estimating evolutionary rate shifts

To gain a general picture of rate variation in melanosome morphology across amniotes, we reconstructed shifts in rates of melanosome evolution including fossil taxa using a Bayesian 'auteur' approach [34] implemented in the rjmcmc.bm function of Geiger [35] (electronic supplementary material, figure S2). We did a phylogenetic PCA with aspect ratio, melanosome length and melanosome diameter using the phyl.resid function in phytools [32] with the 'lambda' model (to account for phylogenetic signal). Principal component 1 explained approximately 90% of the data; therefore, we used this variable in downstream rate shift analyses. We ran two chains for 1 million generations each and assessed convergence with the Gelman–Rubin diagnostic [36].

(ii) Comparing rates of morphological evolution and metabolic rates

To test our first prediction that rates of melanosome shape evolution increase with mass-derived metabolic rate, we used a modified version of the ratebystate function in phytools [32], both with species averages and for black (eumelanin-consistent) and brown (phaeomelanin-consistent) colours separately (R code available at Dryad). We reconstructed ancestral states of mass-derived metabolic rates in extant species using the ace function in ape [37] and computed phylogenetic independent contrasts for melanosome length and diameter at each node. We then combined these univariate contrasts to calculate per-node multivariate distances, or rates [38]. We tested significantly for the relationship between these per-node rates and ancestral estimates of metabolic rate using *p*-values obtained by comparing the observed correlation to a null distribution based on 500 trait evolution simulations [32]. We performed this analysis both in a multivariate framework and with melanosome length and diameter treated separately (see electronic supplementary material, table S2).

(iii) Estimating relationships between morphology and metabolic rate

To test our second prediction that melanosome morphology relates to metabolic rate differently for brown and black colours, we used phylogenetic Bayesian mixed models (BPMMs) implemented in MCMCglmm [39] to account for phylogeny, multivariate response data and repeated measurements within

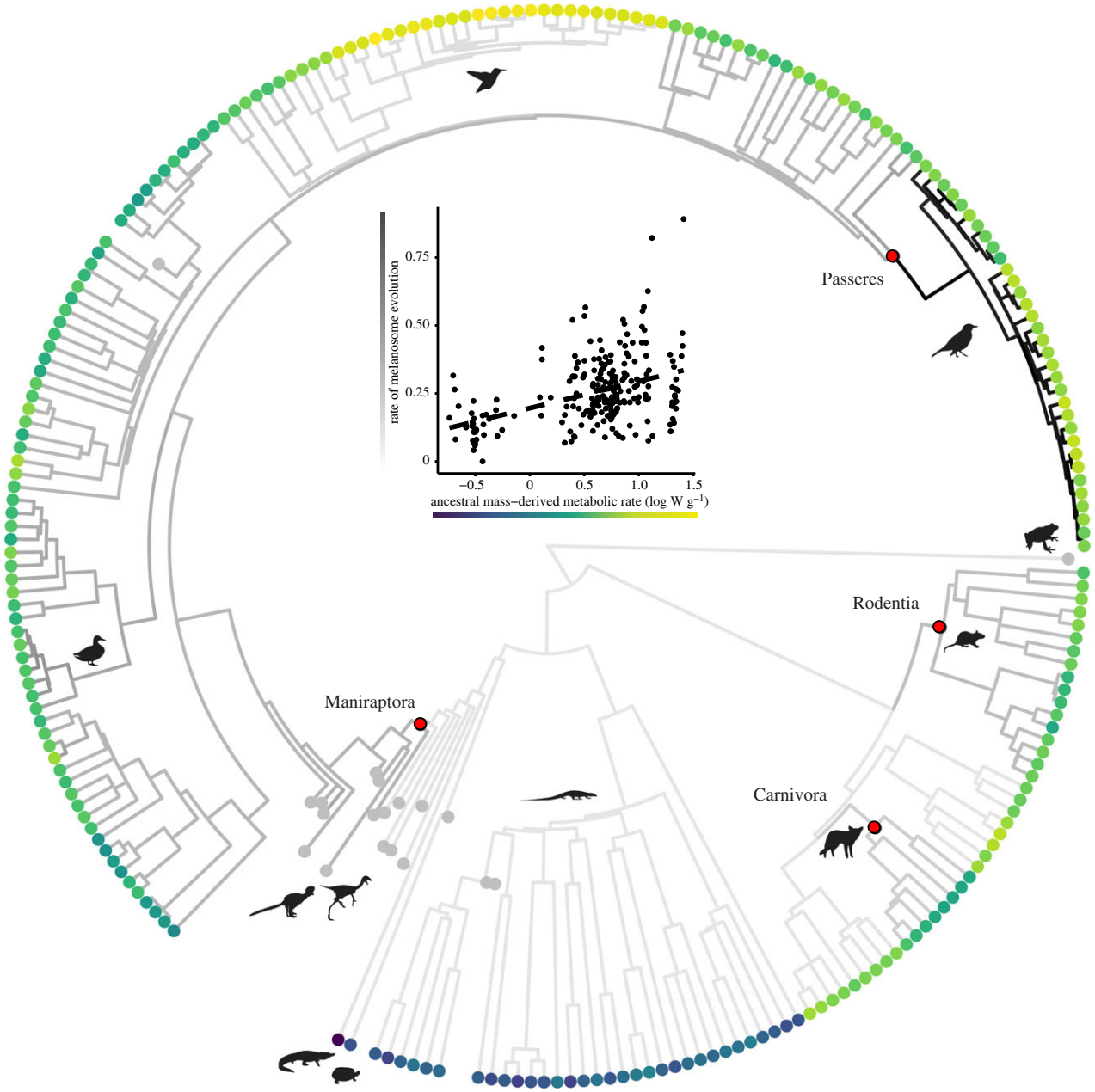

Figure 1. Rates of melanosome shape evolution and variation in metabolic rate across amniotes. Colours of tips correspond to mass-derived metabolic rate (dark blue: low, yellow: high) with fossils in grey. Darker branch colours indicate faster rates of melanosome evolution. Rate shifts are shown as filled circles (red: speed-up, blue: slow-down). Inset shows multivariate phylogenetic contrasts for melanosome morphology versus ancestral metabolic rates ($r = 0.19$, $p_{rand} = 0.006$).

species (e.g. both brown and black colours for some species). We accounted for a model of trait evolution by fitting models using different Ornstein–Uhlenbeck (OU) tree transformations (alpha ranging from 10^{-6} to 10^{-2} in 10 steps) generated with the rescale function [35] and keeping the fit with the lowest DIC scores [40]. We ran separate analyses for three different datasets: (1) a full dataset for species with metabolic rate and/or body mass data ($n = 236$), (2) a dataset limited to only those species with both body mass and metabolic rate data ($n = 77$) and (3) a dataset limited to only species with melanosome data for both black and brown integumentary colours ($n = 31$), analysed with phylogenetic linear models [41]. The latter accounts for uneven sample sizes between black ($n = 134$) and brown integuments ($n = 78$). We then used Wald tests to determine the overall significance of the model (R code on Dryad).

(iv) Clade-specific changes in colour allometry

To test our third prediction that the relationship between melanosome morphology and metabolic rate has changed through time in amniotes, we fitted separate multivariate BPMMs for each subclade to test for clade-specific trends again taking into account phylogenetic signal. We also compared among clade differences in evolutionary rates and covariation among traits in a Bayesian framework using the ratematrix package [42] (see electronic supplementary material, methods for details).

(e) Discriminant function analysis

Given the potential relationship between melanosome morphology and mass-derived metabolic rate, we asked whether accounting for body mass could improve colour reconstruction. We used quadratic discriminant analysis (QDA) to compare two models: one with melanosome length, diameter and aspect ratio as predictors ('no mass' model) and one with body mass, melanosome length, diameter and aspect ratio as predictors ('mass' model). We then compared the prediction performance of these two models using cross-validation tests and self-tests following [14].

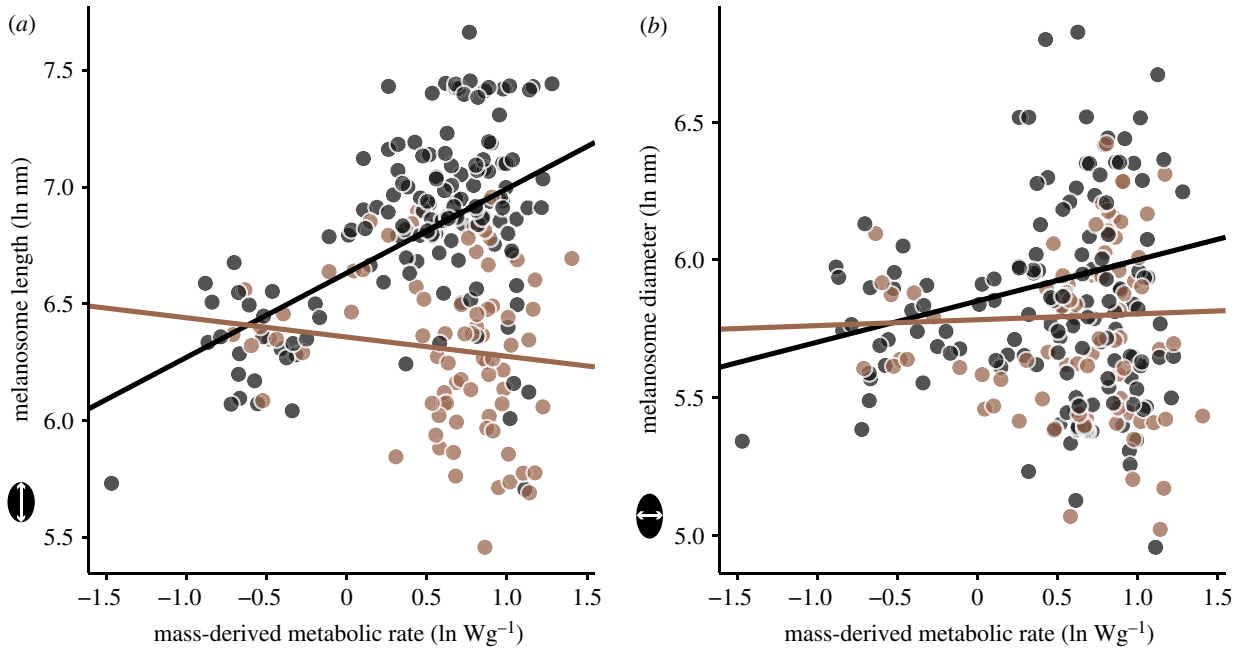

Figure 2. Black and brown integument colours covary with metabolic rate in different ways. Panels show relationships between mass-derived metabolic rate and melanosome length (*a*) and diameter (*b*), for black ($n = 134$) and brown integument colours ($n = 78$). Note the different scales on the *y*-axes. The relationship between metabolic rate and morphology was significant for black (Wald test, $p < 0.001$) but not brown colours ($p = 0.52$).

3. Results

(a) Rates of melanosome shape evolution and metabolism

We identified two increases in the rate of melanosome shape evolution within crown mammals (in Carnivora and Rodentia), an increase at the base of the Maniraptora clade and a subsequent increase within crown birds (Passeres; figure 1). Nodewise rates of melanosome shape evolution increased significantly with metabolic rate (rate-by-state test, $p < 0.01$; see electronic supplementary material, table S2).

(b) Melanic colour system and metabolism

For the full dataset, melanosome length increased with metabolic rate in black (BPMM, $p_{MCMC} < 0.001$) but not brown integuments ($p_{MCMC} = 0.14$, interaction $p_{MCMC} < 0.001$; figure 2*a*; electronic supplementary material, table S3). Melanosome diameter increased significantly with metabolic rate in black ($p_{MCMC} = 0.012$) but not brown integuments ($p_{MCMC} = 0.47$; figure 2*b*). For the metabolic rate-only dataset, the relationship between melanosome morphology and metabolic rate was significant for black (length: $p_{MCMC} < 0.001$, diameter: $p_{MCMC} = 0.046$) but not brown colours (length: $p_{MCMC} = 0.23$, diameter: $p_{MCMC} = 0.51$; electronic supplementary material, figure S6). For the dataset with species having both brown and black colours, the difference in melanosome shape between black and brown integuments increased significantly with higher metabolic rates ($p = 0.037$; electronic supplementary material, figure S7).

(c) Clade-specific changes in colour allometry

Subclade BPMM models revealed colour-specific divergence in the relationship between melanosome length and metabolic rate for mammals (i.e. species with higher metabolic rates have more similar melanosome lengths among black and brown integuments; figure 3*c*) and birds (species with higher metabolic rates have less similar melanosome lengths; figure 3*a*), but not non-avian reptiles (figure 3*e*). Melanosome length was significantly correlated with metabolic rate in brown bird feathers (figure 3*a*), but other subclade relationships were not significant (figure 3*c–f*). For black integuments, multivariate rate analyses showed elevated rates of melanosome shape evolution in birds and mammals compared with non-avian reptiles (posterior overlaps < 0.05; electronic supplementary material, figure S4). Birds also show stronger evolutionary covariation between melanosome length and diameter compared with non-avian reptiles (posterior overlap less than 0.003; electronic supplementary material, figure S4). For brown integuments, rates of melanosome evolution were higher in mammals compared with non-avian reptiles (posterior overlap = 0.032), but other clade comparisons were similar (posterior overlap greater than 0.05; electronic supplementary material, figure S5).

(d) Discriminant function analysis

Incorporating body mass in QDA analyses resulted in 5–6% better performance at predicting colour (electronic supplementary material, table S4).

4. Discussion

We find that rates of melanosome shape evolution increase significantly with metabolic rate. While pleiotropic effects of melanocortins on energetics and colour across vertebrates are long remarked, few studies have assessed broader shifts over macroevolutionary time scales. Qualitative observations have suggested differences between heterotherms and homeotherms in melanosome shape variation [19] and colour-specific shifts in melanosome shape linked to increases in body size [20]. Recent evidence for selection on *Mc1r* suggests a primary role in coloration influenced the evolution of the melanocortin system more than any other member of the *Mc2-5r* groups [43]. Whether physiology is affected by

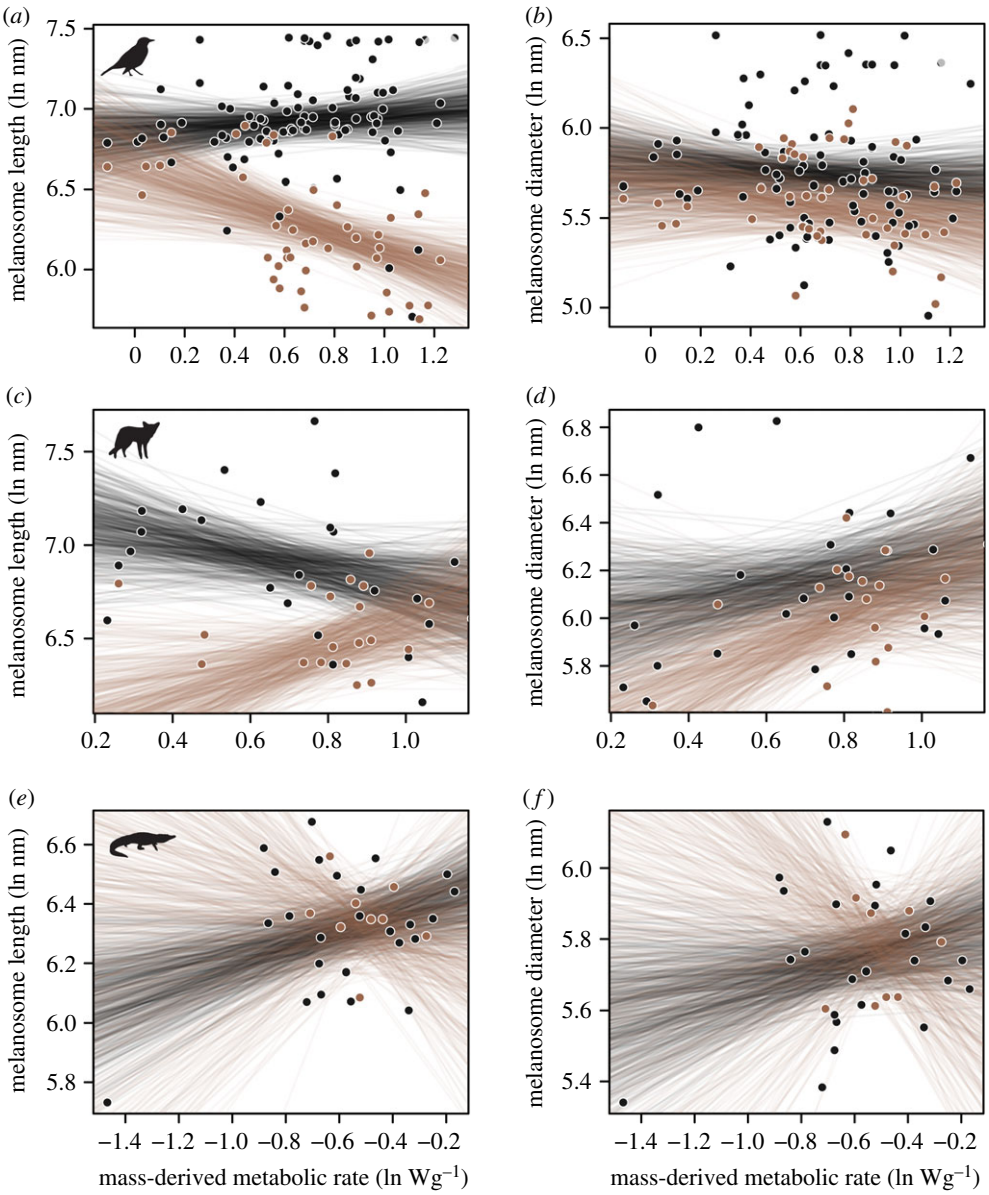

Figure 3. Bayesian phylogenetic mixed models for subclades. Plots show relationships between metabolic rate and (*a*,*c*,*e*) melanosome length and (*b*,*d*,*f*) diameter for different subclades: (*a*,*b*) birds, (*c*,*d*) mammals, (*e*,*f*) non-avian reptiles. Lines indicate integument colour (black or brown), with slopes from a posterior sample of a multivariate MCMCglmm analysis. The relationship between melanosome morphology and metabolic rate is significant for brown feather colours in birds (Wald test, $p = 0.035$). Note the different scales on the axes.

correlated response to selection on *Mc1r* function in coloration or pigmentation evolves under novel energetic regimes remains unclear. However, recent studies in Salamandridae find strong, unambiguous effects on metabolic rate linked to selection for crypsis achieved via the degree of melanization, with a non-trivial 60% increase in SMR attributed to costs of melanogenesis [44]. In nestling barn owls, those with larger dark spots on their wing tips uniformly showed higher metabolic rates than those lacking the spots at the same ambient temperatures [8]. Larger-spotted nestlings also grow faster [45]. Similar to our conclusions here, these authors propose linkages between melanogenesis and energy homeostasis via the melanocortin system.

Body size, metabolic rate shifts and sexual selection are key drivers of morphological evolution [46]. Colour-specific trends between melanosome morphology and metabolic rate (figure 2) suggest that pleiotropy may explain, at least in part, the relationship between rates of morphological evolution and metabolism (figure 1). Birds may express melanocortin receptors in more parts of the body [47] or use melanocortins in more non-colour-related functions, strengthening the relationship between metabolism and melanin-based colour. By contrast, factors such as colour variation driven by genes with few pleiotropic effects (e.g. *Mc1r*) [5], distinct genetic pathways producing similar colour phenotypes (e.g. in birds [48] and mice [49]), or adaptive evolution of melanic colour (e.g. for camouflage) independent of physiology [6] would blur the relationship between metabolism and aspects of the melanic colour system. Heterothermic animals that do not internally regulate their metabolism would be expected to show even less variation in expression of genes involved in energetics (e.g. *POMC*), and interactions between pigment types might further affect colour expression (e.g. *Mc1r* expression mutes the colour effects of *Asip* [48]). Indeed, although *POMC* plays a key role in pigmentation and other melanocortin pathways, a recent study demonstrated only weak coevolutionary relationships with other parts of that pathway [43].

The inclusion of fossils recovers increased rates of melanosome evolution in maniraptoran dinosaurs and coincident with the origin of pinnate feathers [19]. This shift may be consistent with an increase in metabolic rate in the ancestor of this clade. Previously proposed increases in melanosome shape disparity in crown mammals [19]—specifically, in Carnivora and Rodentia (figure 1)—are also recovered. Our analysis also recovers a subsequent rate increase within songbirds (figure 1). These taxa show only slightly higher metabolic rates [23] but shorter lifespans and shorter generation times, factors known to increase evolutionary rates through their effects on mutation rates [46]. Bayesian phylogenetic mixed modelling suggests that a crown bird-specific relationship between melanosome shape and metabolic rate (figure 3*a*) is driving the relationship between ancestral metabolic rates and nodewise rates of melanosome shape evolution (figure 1). Elevated rates of pigment gene evolution in birds and mammals could also explain the increased rates of melanosome evolution in these clades (figure 1; electronic supplementary material, figure S4). Correct estimation of the known colours of extant taxa was improved when accounting for metabolic rate (electronic supplementary material, table S3), a result that may have implications for the clade-specific reconstruction of colour in extinct taxa.

Understanding how morphological traits scale with body size over macroevolutionary timescales is critical for determining whether such scaling acts as a constraint on diversification [50], or if allometry itself evolves [11]—either by natural [51] or sexual selection [52]. Metabolism may limit rates of melanic colour evolution in non-avian reptiles, with a shift in the colour–metabolism relationship expanding the opportunity for rates of colour evolution in maniraptoran dinosaurs (figures 1 and 3*a*). The significant relationship between morphology and metabolic rate for black colours at the overall clade level (figure 2*a*) but not within subclades (figure 3*a*) suggests that 'grade shifts' [53]—coincident changes in multiple traits occurring among major clades—may be driving the pattern across amniotes. The strong bird-specific link between melanosome morphology and metabolic rate for brown colours (figure 3*a*) could be explained by a more prominent role for sexual selection and 'honest' signalling [54] in birds. Alternatively, selection on energetics could have had neutral effects on melanin pigmentation that later became a target of sexual selection. Future work could illuminate whether convergence is seen in *Mc1r* genes in both clades or in other parts of the complex melanocortin system.

Data accessibility. Datasets, phylogenies and R code available on Dryad: http://dx.doi.org/10.5061/dryad.qv871g8 [55].

Authors' contributions. J.A.C. and C.M.E. designed the study and wrote the manuscript; C.M.E. performed analyses.

Competing interests. The authors declare no competing interests.

Funding. This work was supported by a Bass Postdoctoral Fellowship (C.M.E.) and NSF EAR 1251922 (J.A.C.).

Acknowledgements. We wish to thank Jessica Valdes for assistance with data collection, and James Proffitt, Lauren English and Chris Torres for comments on earlier analyses.

References

1. Klingenberg CP. 2004 Integration, modules, and development: molecules to morphology to evolution. In *Phenotypic integration: studying the ecology and evolution of complex phenotypes* (eds M Pigliucci, K Preston), p. 213. New York, NY: Oxford University Press.
2. Gould S, Lewontin R. 1979 The spandrels of San Marco and the Panglossian paradigm: a critique of the adaptationist programme. *Proc. R. Soc. Lond. B* **205**, 581–598. (doi:10.1098/rspb.1979.0086)
3. Cuthill IC *et al.* 2017 The biology of color. *Science* **357**, eaan0221. (doi:10.1126/science.aan0221)
4. Shawkey MD, D'Alba L. 2017 Interactions between colour-producing mechanisms and their effects on the integumentary colour palette. *Phil. Trans. R. Soc. B* **372**, 20160536. (doi:10.1098/rspb.2016.0626)
5. Ducrest A-L, Keller L, Roulin A. 2008 Pleiotropy in the melanocortin system, coloration and behavioural syndromes. *Trends Ecol. Evol.* **23**, 502–510. (doi:10.1016/j.tree.2008.06.001)
6. San-Jose LM, Roulin A. 2018 Toward understanding the repeated occurrence of associations between melanin-based coloration and multiple phenotypes. *Am. Nat.* **192**, 111–130. (doi:10.1086/698010)
7. Kim S-Y, Fargallo JA, Vergara P, Martínez-Padilla J. 2013 Multivariate heredity of melanin-based coloration, body mass and immunity. *Heredity* **111**, 139–146. (doi:10.1038/hdy.2013.29)
8. Dreiss AN, Séchaud R, Béziers P, Villain N, Genoud M, Almasi B, Jenni L, Roulin A. 2016 Social huddling and physiological thermoregulation are related to melanism in the nocturnal barn owl. *Oecologia* **180**, 371–381. (doi:10.1007/s00442-015-3491-3)
9. Roulin A. 2004 Covariation between plumage colour polymorphism and diet in the barn owl *Tyto alba*. *Ibis* **146**, 509–517. (doi:10.1111/j.1474-919x.2004.00292.x)
10. Roskaft E, Jarvi T, Bakken M, Bech C, Reinertsen RE. 1986 The relationship between social-status and resting metabolic-rate in great tits (*Parus major*) and pied flycatchers (*Ficedula hypoleuca*). *Anim. Behav.* **34**, 838–842. (doi:10.1016/S0003-3472(86)80069-0)
11. Uyeda JC, Pennell MW, Miller ET, Maia R, McClain CR. 2017 The evolution of energetic scaling across the vertebrate tree of life. *Am. Nat.* **190**, 185–199. (doi:10.1086/692326)
12. Ito S, Wakamatsu K. 2003 Quantitative analysis of Eumelanin and Pheomelanin in humans, mice, and other animals: a comparative review. *Pigment Cell Res.* **16**, 523–531. (doi:10.1034/j.1600-0749.2003.00072.x)
13. Roulin A, Almasi B, Meichtry-Stier K, Jenni L. 2011 Eumelanin- and pheomelanin-based colour advertise resistance to oxidative stress in opposite ways. *J. Evol. Biol.* **24**, 2241–2247. (doi:10.1111/j.1420-9101.2011.02353.x)
14. Li Q, Gao K-Q, Vinther J, Shawkey MD, Clarke JA, D'Alba L, Meng Q, Briggs DEG, Prum RO. 2010 Plumage color patterns of an extinct dinosaur. *Science* **327**, 1369–1372. (doi:10.1126/science.1186290)
15. Hirobe T, Abe H. 2006 The slaty mutation affects the morphology and maturation of melanosomes in the mouse melanocytes. *Pigment Cell Res.* **19**, 454–459. (doi:10.1111/j.1600-0749.2006.00335.x)
16. Hellström AR *et al.* 2011 Inactivation of Pmel alters melanosome shape but has only a subtle effect on visible pigmentation. *PLoS Genet.* **7**, e1002285. (doi:10.1371/journal.pgen.1002285)
17. Domyan ET *et al.* 2014 Epistatic and combinatorial effects of pigmentary gene mutations in the domestic pigeon. *Curr. Biol.* **24**, 459–464. (doi:10.1016/j.cub.2014.01.020)
18. Santos JC. 2012 Fast molecular evolution associated with high active metabolic rates in poison frogs. *Mol. Biol. Evol.* **29**, 2001–2018. (doi:10.1093/molbev/mss069)
19. Li Q, Clarke JA, Gao K-Q, Zhou C-F, Meng Q, Li D, D'Alba L, Shawkey MD. 2014 Melanosome evolution indicates a key physiological shift within feathered dinosaurs. *Nature* **507**, 350–353. (doi:10.1038/nature12973)
20. Eliason CM, Shawkey MD, Clarke JA. 2016 Evolutionary shifts in the melanin-based color system of birds. *Evolution* **70**, 445–455. (doi:10.1111/evo.12855)
21. Hu D *et al.* 2018 A bony-crested Jurassic dinosaur with evidence of iridescent plumage highlights

complexity in early paravian evolution. *Nat. Commun.* **9**, 217. (doi:10.1038/s41467-017-02515-y)

22. McNamara ME, Orr PJ, Kearns SL, Alcalá L, Anadón P, Mollá EP. 2009 Soft-tissue preservation in Miocene frogs from Libros, Spain: insights into the genesis of decay microenvironments. *Palaios* **24**, 104–117. (doi:10.2110/palo.2008.p08-017r)
23. McKechnie AE, Freckleton RP, Jetz W. 2006 Phenotypic plasticity in the scaling of avian basal metabolic rate. *Proc. R. Soc. B* **273**, 931–937. (doi:10.1098/rspb.2003.2500)
24. White CR, Phillips NF, Seymour RS. 2006 The scaling and temperature dependence of vertebrate metabolism. *Biol. Lett.* **2**, 125–127. (doi:10.1098/rsbl.2005.0378)
25. Makarieva AM, Gorshkov VG, Li B-L, Chown SL, Reich PB, Gavrilov VM. 2008 Mean mass-specific metabolic rates are strikingly similar across life's major domains: evidence for life's metabolic optimum. *Proc. Natl Acad. Sci. USA* **105**, 16 994–16 999. (doi:10.1073/pnas.0802148105)
26. Dunning JB. 2007 *CRC handbook of avian body masses*, 2nd edn. Boca Raton, FL: CRC Press.
27. Jones KE *et al.* 2009 PanTHERIA: a species-level database of life history, ecology, and geography of extant and recently extinct mammals. *Ecology* **90**, 2648. (doi:10.1890/08-1494.1)
28. O'Gorman EJ, Hone DWE. 2012 Body size distribution of the dinosaurs. *PLoS ONE* **7**, e51925. (doi:10.1371/journal.pone.0051925)
29. Pyron RA, Burbrink FT. 2014 Early origin of viviparity and multiple reversions to oviparity in squamate reptiles. *Ecol. Lett.* **17**, 13–21. (doi:10.1111/ele.12168)
30. Burleigh JG, Kimball RT, Braun EL. 2015 Building the avian tree of life using a large-scale, sparse supermatrix. *Mol. Phylogenet. Evol.* **84**, 53–63. (doi:10.1016/j.ympev.2014.12.003)
31. Riede T, Eliason CM, Miller EH, Goller F, Clarke JA. 2016 Coos, booms, and hoots: the evolution of closed-mouth vocal behavior in birds. *Evolution* **70**, 1734–1746. (doi:10.1111/evo.12988)
32. Revell LJ. 2012 phytools: an R package for phylogenetic comparative biology (and other things). *Methods Ecol. Evol.* **3**, 217–223. (doi:10.1111/j.2041-210X.2011.00169.x)
33. Kumar S, Stecher G, Suleski M, Hedges SB. 2017 Timetree: a resource for timelines, timetrees, and divergence times. *Mol. Biol. Evol.* **34**, 1812–1819. (doi:10.1093/molbev/msx116)
34. Eastman JM, Alfaro ME, Joyce P, Hipp AL, Harmon LJ. 2011 A novel comparative method for identifying shifts in the rate of character evolution on trees. *Evolution* **65**, 3578–3589. (doi:10.1111/j.1558-5646.2011.01401.x)
35. Harmon LJ, Weir JT, Brock CD, Glor RE, Challenger W. 2008 GEIGER: investigating evolutionary radiations. *Bioinformatics* **24**, 129–131. (doi:10.1093/bioinformatics/btm538)
36. Gelman A, Rubin DB. 1992 Inference from iterative simulation using multiple sequences. *Stat. Sci.* **7**, 457–472. (doi:10.1214/ss/1177011136)
37. Paradis E, Claude J, Strimmer K. 2004 APE: analyses of phylogenetics and evolution in R language. *Bioinformatics* **20**, 289–290. (doi:10.1093/bioinformatics/btg412)
38. McPeek MA, Shen L, Torrey JZ, Farid H. 2008 The tempo and mode of three-dimensional morphological evolution in male reproductive structures. *Am. Nat.* **171**, E158–E178. (doi:10.1086/587076)
39. Hadfield JD, Nakagawa S. 2010 General quantitative genetic methods for comparative biology: phylogenies, taxonomies and multi-trait models for continuous and categorical characters. *J. Evol. Biol.* **23**, 494–508. (doi:10.1111/j.1420-9101.2009.01915.x)
40. Tobias JA, Cornwallis CK, Derryberry EP, Claramunt S, Brumfield RT, Seddon N. 2014 Species coexistence and the dynamics of phenotypic evolution in adaptive radiation. *Nature* **506**, 359–363. (doi:10.1038/nature12874)
41. Ho L, Ané C. 2014 A linear-time algorithm for Gaussian and non-Gaussian trait evolution models. *Syst. Biol.* **63**, 397–408. (doi:10.1093/sysbio/syu005)
42. Caetano DS, Harmon LJ. 2017 ratematrix: an R package for studying evolutionary integration among several traits on phylogenetic trees. *Methods Ecol. Evol.* **8**, 1920–1927. (doi:10.1111/2041-210X.12826)
43. Dib L, San-Jose LM, Ducrest A-L, Salamin N, Roulin A. 2017 Selection on the major color gene melanocortin-1-receptor shaped the evolution of the melanocortin system genes. *Int. J. Mol. Sci.* **18**, 2618. (doi:10.3390/ijms18122618)
44. Polo-Cavia N, Gomez-Mestre I. 2017 Pigmentation plasticity enhances crypsis in larval newts: associated metabolic cost and background choice behaviour. *Sci. Rep.* **7**, 39739. (doi:10.1038/srep39739)
45. Almasi B, Roulin A. 2015 Signalling value of maternal and paternal melanism in the barn owl: implication for the resolution of the lek paradox. *Biol. J. Linn. Soc.* **115**, 376–390. (doi:10.1111/bij.12508)
46. Cooper N, Purvis A. 2009 What factors shape rates of phenotypic evolution? A comparative study of cranial morphology of four mammalian clades. *J. Evol. Biol.* **22**, 1024–1035. (doi:10.1111/j.1420-9101.2009.01714.x)
47. Ling MK, Hotta E, Kilianova Z, Haitina T, Ringholm A, Johansson L, Gallo-Payet N, Takeuchi S, Schiöth HB. 2004 The melanocortin receptor subtypes in chicken have high preference to ACTH-derived peptides. *Br. J. Pharmacol.* **143**, 626–637. (doi:10.1038/sj.bjp.0705900)
48. Uy JAC, Cooper EA, Cutie S, Concannon MR, Poelstra JW, Moyle RG, Filardi CE. 2016 Mutations in different pigmentation genes are associated with parallel melanism in island flycatchers. *Proc. R. Soc. Lond. Ser. B* **283**, 20160731. (doi:10.1007/s00265-013-1492-y)
49. Kingsley EP, Manceau M, Wiley CD, Hoekstra HE. 2009 Melanism in *Peromyscus* is caused by independent mutations in agouti. *PLoS ONE* **4**, e6435. (doi:10.1371/journal.pone.0006435.s003)
50. West GB, Brown JH. 2005 The origin of allometric scaling laws in biology from genomes to ecosystems: towards a quantitative unifying theory of biological structure and organization. *J. Exp. Biol.* **208**, 1575–1592. (doi:10.1242/jeb.01589)
51. Skandalis DA *et al.* 2017 The biomechanical origin of extreme wing allometry in hummingbirds. *Nat. Commun.* **8**, 1047. (doi:10.1038/s41467-017-01223-x)
52. Kodric-Brown A, Sibly RM, Brown JH. 2006 The allometry of ornaments and weapons. *Proc. Natl Acad. Sci. USA* **103**, 8733–8738. (doi:10.1073/pnas.0602994103)
53. Garland T. 2014 Trade-offs. *Curr. Biol.* **24**, R60–R61. (doi:10.1016/j.cub.2013.11.036)
54. Jawor J, Breitwisch R. 2003 Melanin ornaments, honesty, and sexual selection. *The Auk* **120**, 249–265. (doi:10.1642/0004-8038(2003)120[0249:MOHASS]2.0.CO;2)
55. Eliason CM, Clarke JA. 2018 Data from: Metabolic physiology explains macroevolutionary trends in the melanic colour system across amniotes. Dryad Digital Repository. (doi:10.5061/dryad.qv871g8)